Photoluminescence decay dynamics of noninteracting silicon nanocrystals

ARTICLE *in* JOURNAL OF APPLIED PHYSICS · APRIL 2004

Impact Factor: 2.18 · DOI: 10.1063/1.1652245 · Source: OAI

Photoluminescence decay dynamics of noninteracting silicon nanocrystals

O. Guillois, N. Herlin-Boime, and C. Reynaud[a)]
Laboratoire Francis Perrin (URA CEA-CNRS 2453), Service des Photons Atomes et Molécules, DSM/DRECAM CEA-Saclay, F-91191 Gif/Yvette Cedex France

G. Ledoux[b)] and F. Huisken
Max-Planck-Institut für Strömungsforschung, Bunsenstraße 10, D-37073 Göttingen, Germany

(Received 21 October 2003; accepted 8 January 2004)

Time-resolved photoluminescence measurements on size-selected silicon nanocrystals have been carried out in order to elucidate the nonexponential behavior of the photoluminescence decay kinetics. The nanoparticles are gas-phase synthesized, extracted as a supersonic beam, size selected, and deposited downstream as films of variable densities. The nanoparticle number densities were determined by atomic force microscopy. The photoluminescence properties appear totally independent of the film density. Even in the very low density film where nanoparticles are completely isolated from each other, the decay kinetics corresponds to a stretched exponential law. This means that the stretched exponential kinetics does not originate from the interaction between nanoparticles, but is actually a characteristic of the silicon nanocrystals. © *2004 American Institute of Physics.* [DOI: 10.1063/1.1652245]

I. INTRODUCTION

Light-emitting silicon nanocrystals (*nc*-Si) have attracted much interest due to their importance for optoelectronic devices. This interest is reinforced by the fact that the photoluminescence (PL) intensity can be very strong at room temperature. In spite of the great number of fundamental studies devoted to the understanding of PL properties, there is still a lively debate about its origin. Because the PL energy peak is found to be size dependent in the majority of cases, electron-hole recombination in a quantum confined system is generally considered as the theoretical frame explaining the PL properties. However, there is a debate regarding the role played by the surface states and by the interaction with the surroundings or between the nanoparticles.

This is particularly true for the temporal PL behavior. The decay is not single exponential but takes place more slowly than exponential. Decay curves well described by a stretched exponential law have been systematically reported for all types of nanocrystalline silicon.[1–9] Such decay kinetics is expected when there are several pathways of deexcitation with different characteristic times, and generally indicates a significant disorder in the material. This behavior was also observed in other systems, for example in ZnSe-ZnTe superlattices,[10] in SiO_2 with oxygen-deficient-type defects,[11] in amorphous carbon,[12] in polymers,[13] as well as in chromophore-solvent systems.[14] The stretched exponential function provides a good empirical fit, but has no physical significance.[15] A two-state model for subexponential fluorescence has been proposed, where the fluorescing level is fed by a trapped state.[16] The stretched exponential decay is then explained by a simple detrapping process localized in the vicinity of the fluorescing center, with a distribution of detrapping rates due to variations in the local environments. In a recent paper[17] reporting numerical simulations on trapping-controlled luminescence, it was shown that the stretched exponential function is able to describe the decay of luminescence in an ordered crystal, as well.

In the case of silicon nanostructures (porous silicon or silicon nanocrystals embedded in silica matrices), the origin of the stretched exponential decay is often attributed to interactions between the nanocrystals, with excitation transfer from the smaller particles to the bigger ones.[3,5,7] Due to the possibly large distribution of interparticle distances and particle sizes, this explanation has been adopted by various authors, because it seems able to explain the strong nonexponential character of the PL decay observed in several samples. In contrast to these approaches assuming a hopping mechanism as the origin for the stretched exponential, the absence of carrier hopping has been demonstrated experimentally in porous silicon[18] and theoretically in the framework of a two-state model involving a trapped state.[16] Alternatively, a distribution of radiative and/or nonradiative rates could explain the stretched exponential decay. In the case of radiative recombination, it has been shown theoretically that the rate is sensitive to the geometry of the nanocrystals.[19,20] Also, since silicon is an indirect-band-gap semiconductor, the radiative process is phonon assisted, and the radiative rate depends significantly on the type and number of phonons involved in the process.[19,21] In the case of nonradiative processes, it is reasonable to invoke a distribution of defect radii.

In the case of films made from gas phase grown silicon nanocrystals,[22,6] the PL measurements do not indicate any contribution from excitation transfer processes. Indeed, samples with low densities of size-selected nanocrystals have been studied, and the decay kinetics appears to be nonexponential as well. In order to elucidate this question, we de-

[a)]Electronic mail: creynaud@drecam.cea.fr
[b)]Present address: Laboratoire de Physico Chimie des Materiaux Luminescents, Université Claude Bernard, 43 boulevard du Novembre 1918, 69622 Villeurbanne Cedex France.

cided to prepare *nc*-Si films with systematic variation of the nanocrystal density and to study in detail the PL decay behavior. Time-resolved PL measurements have been performed and are reported and discussed in this paper.

II. EXPERIMENT

The samples studied in this work were synthesized by laser pyrolysis of silane in a gas flow reactor. A complete description of the apparatus has been presented earlier.[22] Briefly, a pulsed CO_2 laser irradiates a laminar flow of silane, causing the total decomposition of the molecules and giving rise to the formation of silicon clusters and nanoparticles. A conical nozzle is placed near the reaction center and extracts a small part of the clusters which are skimmed into a low pressure differential chamber to form a molecular beam of noninteracting Si nanoparticles. A rotating chopper synchronized with the pulsed CO_2 laser intercepts the beam and allows the separation of cluster sizes in space.[23] They can then be deposited on any substrate for further studies. The size distribution of the clusters is determined *in situ* by time-of-flight mass spectrometry (TOFMS). Four samples were prepared on a single day, one after the other without interrupting the vacuum. The experimental conditions of the pyrolysis summarized here were kept strictly constant: flow of silane, 28 SCCM (where SCCM denotes cubic centimeter per minute at STP); flow of helium, 1100 sccm; total pressure, 330 mbar; CO_2 laser line, 10 μP28 (936.8 cm^{-1}); laser energy, 35 mJ/pulse; pulse length, 20 ns; repetition rate, 20 Hz. Samples were deposited on fused quartz substrates. The only variable parameter was the deposition time, which was fixed successively to 5, 50, 500, and 5000 s. These samples are designated in the following by A, B, C, and D, respectively. The size distribution of the particles in the beam was controlled by TOFMS. These measurements were made before the first as well as after the third and fourth depositions. The average particle size appeared quite stable at a value of 3.4 nm for samples A, B, and C, and evolved slightly from 3.40 up to 3.46 during the longest deposition (D). The width of the size distribution gradually changed from 0.7 to 0.85 nm during the entire deposition experiment. All four samples were analyzed by atomic force microscopy (AFM) in order to check the morphology of the deposit and to determine the particle number density. The AFM apparatus was a multimode scanning probe microscope from Digital Instruments used in the tapping mode.

The PL properties of these samples were measured with a home-made experimental setup described in detail elsewhere.[6] The fourth harmonic (266 nm) of a pulsed neodymium-doped yttrium aluminum garnet (Nd:YAG) laser was used as the exciting source. The laser was operated at a repetition rate of 15 Hz with a pulse width of 4 ns. The beam was filtered by UG 11 filters to discriminate against the other harmonics (532 nm and fundamental). A beam splitter sent part of the beam to a control diode which monitored the incident power. The PL was detected by an optical setup made of a lens, a monochromator, and a photomultiplier (Hamamatsu R928, with Peltier cooling). The absorption of samples at the laser wavelength (266 nm) was determined in a separate experiment. Our aim was to measure the PL spectrum, the PL yield, and the decay kinetics as a function of the deposition time of the samples. The detection setup was calibrated with a tungsten ribbon lamp. All the PL measurements were made at very low laser fluence (50 $\mu J/cm^2$) in order to avoid nonlinear effects.[8] The signal from the photomultiplier was sent to a numerical oscilloscope synchronized with the laser and averaged for a given number of laser pulses. The time trace was recorded with a resolution of 100 ns. The laser pulse is short compared to the PL average lifetimes of our samples ($\sim$100 μs) and can be considered as instantaneous. The intensity given for each wavelength in the PL spectrum was determined by integrating this time trace over 2 ms. Alternatively, at very low signal level, a multichannel analyzer was used in the counting mode.

III. RESULTS AND DISCUSSION

In order to determine the number densities of the deposits, all four samples were analyzed with the AFM. The corresponding micrographs are shown in Fig. 1. Note that the analysis was done on exactly the same samples that were prepared for the PL study, i.e., the substrate was quartz and not mica which would have been more appropriate. This explains why the images shown in Fig. 1 are not so good as usual,[24] but for the present purpose, the quality is sufficient. The images were taken at the centers of the samples, on the day following the synthesis. As expected, the particle density on the substrate seems to correlate with the deposition time. For the shortest times (samples A and B), one can clearly see that the particles are well separated from each other and do not interact. This is no longer true for the two other samples, particularly for sample D where the accumulation inevitably causes direct contact of the particles.

From these AFM images, it is also possible to determine the number densities of the nanoparticles. The best candidate for this analysis is sample B, where the density is high enough to obtain sufficient statistics, but low enough to avoid particle superposition. For this sample, we determined a number density of 3.8×10^{10} particles/cm^2. Because the experimental conditions were maintained constant for all the deposits, we derive a 100 times higher number density for sample D, namely, 3.8×10^{12} particles/cm^2. A proof of the correctness of this extrapolation is given by the PL measurements (see below).

All samples are optically thin even at the UV excitation wavelength used here for the PL measurements (266 nm). For the thickest sample (D), the transmission could be measured with reliable precision. After an independent measurement of the transmission of the substrate alone, the absorption of the nanoparticle deposit was found to be 7%. The contribution of reflection is assumed to be negligible. The absorption coefficient of the *nc*-Si layer at 266 nm can be estimated, since we know the particle number density from AFM analysis, as well as the average particle size from TOFMS. The particles can be considered as spherical.[25] However, due to the contact with the ambient atmosphere, the silicon particles undergo oxidation and are subjected to an aging phenomenon.[25,26] The oxidation leads to the appear-

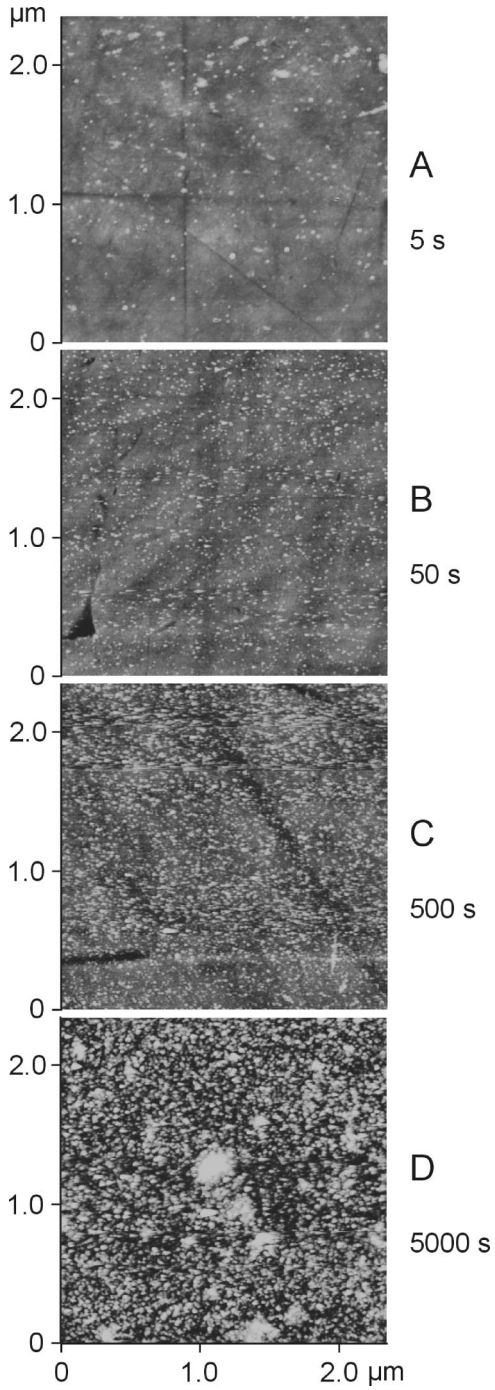

FIG. 1. Atomic force microscopy images of four deposits of *nc*-Si particles produced by laser pyrolysis and deposited on quartz substrates. The four samples were produced on a single day under rigorously the same experimental conditions. The only variable parameter from one sample to the other was the deposition time (5, 50, 500, and 5000 s for samples A, B, C, and D, respectively).

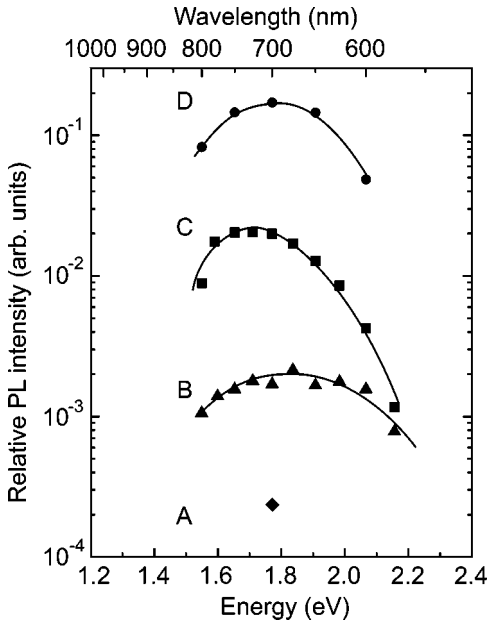

FIG. 2. Relative PL energy distributions for samples A, B, C, and D. Each data point corresponds to the PL intensity as measured in a 7-nm-wide window centered at the given wavelength. The solid lines are guides for the eyes.

ance of the PL due to its role in the passivation of dangling bonds at the silicon surface, but is a self-limited process.[25] After full passivation, the diameter of the crystalline core is reduced by a factor of 0.87 compared to its original value.[6] Thus, the average diameter is reduced from 3.5 to 3 nm in the present samples. With this value, the effective thickness of the silicon layer of sample D becomes 0.54 nm, and the absorption coefficient of the silicon nanocrystals at 266 nm is calculated to be $\alpha = 1.3 \times 10^6$ cm^{-1}. Note that this is an overestimated value due to the neglect of reflection. Nevertheless, this result can be compared with the values reported for bulk Si [2×10^6 cm^{-1} (Ref. 27)], and for porous silicon with 79% porosity [1×10^6 cm^{-1} (Ref. 28)].

The PL intensity measured for the different samples is reported in Fig. 2. In the case of samples A and B, the signal is very weak due to the very low particle density on the substrate. Thus, only the region around the PL maximum could be studied for sample A, and the signal-to-noise ratio is rather low for sample B. Nevertheless, the variation of the PL intensity with the emission wavelength appears similar for all samples. In agreement with previous results obtained with similar size distributions,[6] the maximum is around 700 nm. The most remarkable result taken from Fig. 2 is that the spectra are separated from each other by exactly one decade, demonstrating a very good relationship with the deposition times which differ by a factor of 10. This is the first strong indication that the PL process is not sensitive to the nanoparticle density in these samples.

A direct evaluation of the PL yield is possible from these measurements. Indeed, the laser beam was focused to a 0.3 mm diameter spot on the sample, so that the number of illuminated nanoparticles was 2.7×10^9 for sample D. The laser fluence was 50 μJ/cm^2, corresponding to 4.7×10^{10} photons on the laser spot. The number of absorbed photons was 7% at maximum, i.e., 3.3×10^9 photons. Therefore, the average number of photons absorbed by each Si nanoparticle did not exceed 1.2. Roughly, each nanoparticle absorbed one photon per pulse. Under these conditions, saturation effects were largely avoided.[8] The number of emitted photons per pulse, integrated over the whole measured wavelength range, was measured to be 3×10^8. Therefore, the number of photons

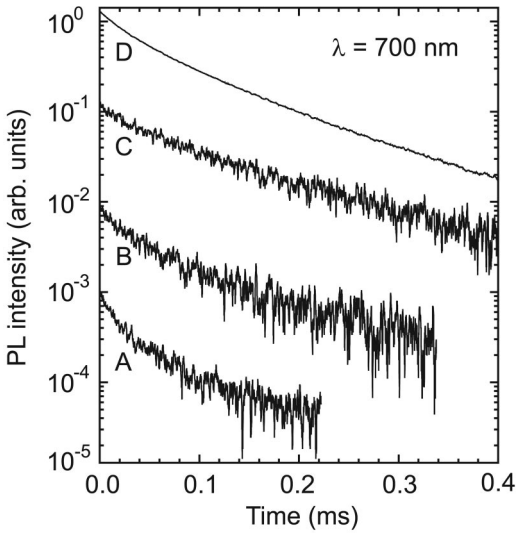

FIG. 3. Comparison between the decay curves of the photoluminescence measured at 700 nm for the four samples. For clarity, the normalized curves were separated by one decade each.

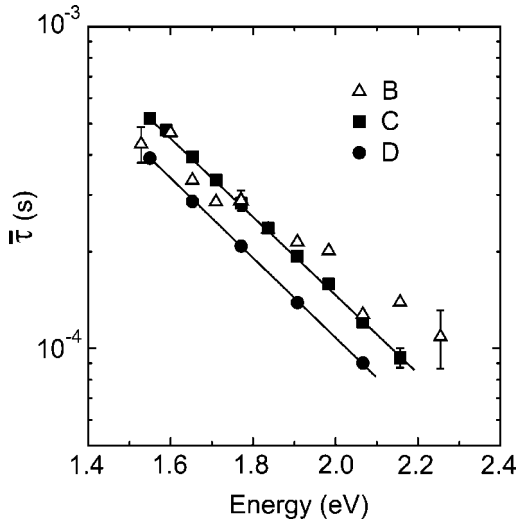

FIG. 4. Average lifetime $\overline{\tau}$ values for the three samples B, C, and D at different PL energies. The solid lines represent linear fits to the data points of sample C and D.

emitted by each particle was 0.11. Thus, the PL yield is calculated to be 9% for all samples.

The PL decay curves are reported in Fig. 3 for all four samples. They were recorded at the same PL wavelength of 700 nm where the signal was highest. The PL decay kinetics extends over a long time scale, the decay times remaining long because silicon, even if nanostructured, conserves its indirect band gap character with rather slow phonon-assisted transitions.[29,21] Clearly, the temporal behavior of the PL process is the same in all samples and does not depend on the particle density on the substrate. Also, the curves cannot be represented by a single exponential, rather they exhibit a nonexponential decay. All curves can be fitted by a stretched exponential function

$$I_{\mathrm{PL}}(t) = I_0 \exp[-(t/\tau)^{\beta}], \tag{1}$$

where τ is the lifetime and β the dispersion factor. In this function, the parameter β can take values between 0 and 1. For $\beta = 1$, the decay is single exponential and, in this case, τ is simply the regular PL lifetime. The more β deviates from 1, the more the decay curve acquires a nonexponential character. An average decay time $\overline{\tau}$ can be defined by

$$\overline{\tau} = \frac{1}{I_0}\int_0^{\infty} I_{\mathrm{PL}}(t)\,dt. \tag{2}$$

Note that $\overline{\tau}$ represents the time at which half of the energy has been emitted. Integrating the stretched exponential law, we obtain

$$\overline{\tau} = \tau \frac{1}{\beta}\Gamma\left(\frac{1}{\beta}\right), \tag{3}$$

where Γ is the gamma function. In Fig. 4, the values of $\overline{\tau}$, obtained by fitting the decay curves measured at various wavelengths by stretched exponentials, are reported for each sample as a function of the PL emission energy. The variations are very similar for all samples. The $\overline{\tau}$ values range from 100 to 500 μs and decrease exponentially when the PL energy is increased. This variation of $\overline{\tau}$ with the PL energy is well known for all nanocrystalline forms of silicon. Indeed, when the gap of the nanoparticles increases, the radiative recombination rate increases, due to an enhanced quantum confinement.[21] Since, in general, the nonradiative rates are much less sensitive to the gap, the consequence is a decrease of the corresponding PL lifetime. The parameter β is roughly constant with the PL energy and takes values between 0.6 and 0.7. This means that the phenomenon responsible for the stretched exponential decay is not strongly affected by the gap value.

The interesting point is that the decay behavior is independent of the particle density on the substrate and that, even in the very diffuse films of samples A and B, the decay exhibits a stretched exponential shape. Therefore, we conclude that the nonexponential decay behavior cannot result from an excitation transfer between the nanoparticles. Otherwise, the decay curves would not be the same in samples A and D.

It is worthwhile to discuss in more detail the data displayed in Fig. 4. While the data are very similar for all samples, there is a small discrepancy between the data from sample D and the others. Indeed, these data were recorded at different times after sample synthesis, and as mentioned above, due to the oxidation, the silicon particles were subjected to an aging phenomenon.[25,26] At the very beginning, the PL spectrum increases strongly in intensity, broadens, and shifts to the blue. On long-term observation, it seems that only the PL intensity continues to increase, and, at the same time, the PL decay time increases too. Because sample D was measured one month earlier, its decay time was determined to be somewhat smaller than that of the others. Carrying out a spot check at one wavelength and measuring the decay of all samples at the same time, we confirmed that the decay behavior is the same in all samples. The variation of the decay time with aging and its correlation with the PL yield will be detailed in a forthcoming paper.

It should be stressed that our Si nanoparticles are sur-

rounded by a 0.35-nm-thick layer of SiO_2. Thus, the nanocrystals are always separated by a distance of at least 0.7 nm. Therefore, it cannot be excluded that, in other kinds of nanostructured Si materials, excitation transfer could be operative, in particular if the nanocrystals come closer to each other. But the present results show that excitation transfer alone cannot explain the stretched exponential decay and that other processes must be involved.

Now we want to discuss our findings with the results obtained for porous silicon (p-Si).[18] In previous papers,[6,8] the close similarity between the PL of the present nc-Si and p-Si samples has already been emphasized. Therefore, it is very likely that the PL decay is governed by the same mechanisms. In p-Si, the emitting nanocrystalline structures can be considered to be in close contact to each other. Nevertheless, the parameters $\overline{\tau}$ and β deduced from time-resolved PL measurements on p-Si are not very different from those obtained from our nc-Si films.[8] Thus, excitation transfer between particles is probably also not operative in p-Si. This is in full agreement with the paper of Mihalcescu *et al.*,[18] in which the absence of carrier hopping between different localized states was demonstrated. Therefore, the luminescent centers in p-Si must be considered as independent and the recombination mechanism as a local competition between radiative and nonradiative electron-hole pair recombination. The same conclusion can be drawn here in the case of gas phase synthesized nc-Si. This result also supports the theoretically based conclusions of Huber *et al.*[16] that it is not necessary to invoke hopping mechanisms in order to explain the stretched exponential kinetics. Instead, it is sufficient to consider the simple two-state model where the fluorescing level is fed by a trapped state and where we have a distribution of detrapping rates across the solid, due to variations in the local environments.

The samples studied in the present paper were size selected with a fairly narrow size distribution. Therefore, the behavior of samples with much broader size distribution is questionable. Several samples have been studied with different size distributions[6] or deposited without size selection,[9] but the size distribution does not appear as a parameter influencing the PL decay kinetics.

The origin of the stretched exponential decay must be linked to an actual characteristic of the nc-Si particle. It has been demonstrated by high resolution transmission electron microscopy[25] that the silicon lattice parameter is a function of the crystallite size, and that for a given size there is a distribution of lattice parameters. This result has been interpreted as being due to the effect of the silicon oxide shell on the nc-Si core. The oxidation process leads to an amorphous SiO_2 layer whose thickness and structure are somewhat different from one particle to another. The pressure exerted by this layer on the crystal lattice is therefore different. This effect has been invoked recently[6] to explain the inhomogeneous character of the PL bandwidth of a size-selected sample. It can be expected that this lattice effect has an even more pronounced influence on the radiative lifetime. Indeed, such effect could be considered as similar to the geometry effect demonstrated theoretically.[19,20] Finally, the dependence of the radiative recombination rate on the type and number of phonons involved in the phonon-assisted process[19,21] leads to a scattering of the radiative rates at a given energy and could be an intrinsic effect responsible for the stretched exponential decay in silicon nanocrystals.

IV. CONCLUSION

Time-resolved photoluminescence measurements on size-selected silicon nanocrystals have given detailed insight into the stretched exponential behavior of the PL decay. The PL properties appear totally independent of the film density in the case of gas-phase-grown nc-Si. Even in the very low density film, where nanoparticles are completely isolated from each other, the decays exhibit a stretched exponential shape. This means that the stretched exponential decay does not result from an interparticle interaction. Instead, the luminescent centers must be considered as independent and the recombination mechanism as a local competition between radiative and nonradiative electron-hole pair recombination. The variation of the atomic structure of the oxidized nc-Si nanoparticle could be the origin of the distribution of process rates responsible for the stretched exponential behavior of the PL decay. The intrinsic distribution of radiative recombination rates due to the phonon-assisted character of this process in silicon could also contribute.

ACKNOWLEDGMENTS

This work was supported by the European Commission (IST-SINERGIA) and PROCOPE, a bilateral cooperation between France and Germany. One of the authors (G.L.) acknowledges the support of the Alexander von Humboldt foundation.

[1] X. Chen, B. Henderson, and K. P. O'Donnel, Appl. Phys. Lett. **60**, 2672 (1992).
[2] E. Bustarret, I. Mihalcescu, M. Ligeon, R. Romestain, J. C. Vial, and F. Madeore, J. Lumin. **57**, 105 (1993).
[3] L. Pavesi and M. Ceschini, Phys. Rev. B **48**, 17625 (1993).
[4] I. Mihalcescu, J. C. Vial, and R. Romestain, J. Appl. Phys. **80**, 2404 (1996).
[5] J. Linnros, N. Lalic, A. Galeckas, and V. Grivickas, J. Appl. Phys. **86**, 6128 (1999).
[6] G. Ledoux, O. Guillois, F. Huisken, B. Kohn, V. Paillard, D. Porterat, and C. Reynaud, Phys. Rev. B **62**, 15 942 (2000).
[7] F. Priolo, G. Franzo, D. Pacifici, V. Vinciguerra, F. Iacona, and A. Irrera, J. Appl. Phys. **89**, 264 (2001).
[8] D. Amans, O. Guillois, G. Ledoux, D. Porterat, and C. Reynaud, J. Appl. Phys. **91**, 5334 (2002).
[9] F. Huisken, G. Ledoux, O. Guillois, and C. Reynaud, Adv. Mater. (Weinheim, Ger.) **14**, 1861 (2002).
[10] K. Suzuki *et al.*, Solid State Commun. **105**, 571 (1998).
[11] N. Nishikawa *et al.*, J. Non-Cryst. Solids **222**, 221 (1997).
[12] W. Lormes, M. Hundhausen, and L. Ley, J. Non-Cryst. Solids **227–230**, 570 (1998).
[13] B. Dulieu, J. Wery, S. Lefrant, and J. Bullot, Phys. Rev. B **57**, 9118 (1998).
[14] A. Kurita, K. Matsumoto, Y. Shibata, and T. Kushida, J. Lumin. **76**, 295 (1998).
[15] I. Kuskovsky, G. F. Neumark, V. N. Bondarev, and P. V. Pikhitsa, Phys. Rev. Lett. **80**, 2413 (1998).
[16] D. L. Huber, J. Lumin. **86**, 95 (2000); J. Garcia-Adeva and D. L. Huber, *ibid.* **92**, 65 (2000).
[17] R. Chen, J. Lumin. **102–103**, 510 (2003).
[18] I. Mihalcescu, J. C. Vial, and R. Romestain, Phys. Rev. Lett. **80**, 3392 (1998).
[19] M. S. Hybertsen, Phys. Rev. Lett. **72**, 1514 (1994).

[20] L. W. Wang and A. Zunger, J. Phys. Chem. **98**, 2158 (1994).
[21] C. Delerue, G. Allan, and M. Lannoo, Phys. Rev. B **64**, 193402 (2001).
[22] M. Ehbrecht and F. Huisken, Phys. Rev. B **59**, 2975 (1999).
[23] G. Ledoux, J. Gong, F. Huisken, O. Guillois, and C. Reynaud, Appl. Phys. Lett. **80**, 4834 (2002).
[24] F. Huisken, H. Hofmeister, B. Kohn, M. A. Laguna, and V. Paillard, Appl. Surf. Sci. **154–155**, 305 (2000).
[25] H. Hofmeister, F. Huisken, and B. Kohn, Eur. Phys. J. D **9**, 137 (1999).
[26] G. Ledoux, J. Gong, and F. Huisken, Appl. Phys. Lett. **79**, 4028 (2001).
[27] D. F. Edwards, in *Handbook of Optical Constants of Solids*, edited by E. D. Palik (Academic Press, Orlando, FL, 1985), Vol. I, p. 547; *ibid.* Vol. III, p. 531.
[28] W. Theiss, Surf. Sci. Rep. **29**, 91 (1997).
[29] C. Delerue, G. Allan, and M. Lannoo, Phys. Rev. B **48**, 11024 (1993).